Progressive hearing loss and gradual deterioration of sensory hair bundles in the ears of mice lacking the actin-binding protein Eps8L2

David N. Furness[a,1], Stuart L. Johnson[b,1], Uri Manor[c,1], Lukas Rüttiger[d,1], Arianna Tocchetti[e,2], Nina Offenhauser[e], Jennifer Olt[b], Richard J. Goodyear[f], Sarath Vijayakumar[g], Yuhai Dai[c], Carole M. Hackney[b], Christoph Franz[d], Pier Paolo Di Fiore[e,h,i], Sergio Masetto[j], Sherri M. Jones[g], Marlies Knipper[d], Matthew C. Holley[b], Guy P. Richardson[f], Bechara Kachar[c], and Walter Marcotti[b,3]

[a]Institute for Science and Technology in Medicine, Keele University, Keele ST5 5BG, United Kingdom; [b]Department of Biomedical Science, University of Sheffield, Sheffield S10 2TN, United Kingdom; [c]Laboratory of Cell Structure and Dynamics, National Institute on Deafness and Other Communication Disorders, National Institutes of Health, Bethesda, MD 20892; [d]Department of Otolaryngology, Tübingen Hearing Research Centre (THRC), University of Tübingen, 72076 Tübingen, Germany; [e]Fondazione Istituto FIRC di Oncologia Molecolare (IFOM), 20139 Milan, Italy; [f]School of Life Sciences, University of Sussex, Brighton BN1 9QG, United Kingdom; [g]Department of Special Education and Communication Disorders, University of Nebraska, Lincoln, NE 68583; [h]Istituto Europeo di Oncologia, 20141 Milan, Italy; [i]Dipartimento di Scienze della Salute, Universita' degli Studi di Milano, 20122 Milan, Italy; and [j]Department of Physiological and Pharmacological Science, University of Pavia, Pavia 27100, Italy

Edited by Michael Deans, Johns Hopkins University, Baltimore, MD, and accepted by the Editorial Board July 8, 2013 (received for review March 13, 2013)

Mechanotransduction in the mammalian auditory system depends on mechanosensitive channels in the hair bundles that project from the apical surface of the sensory hair cells. Individual stereocilia within each bundle contain a core of tightly packed actin filaments, whose length is dynamically regulated during development and in the adult. We show that the actin-binding protein epidermal growth factor receptor pathway substrate 8 (Eps8)L2, a member of the Eps8-like protein family, is a newly identified hair bundle protein that is localized at the tips of stereocilia of both cochlear and vestibular hair cells. It has a spatiotemporal expression pattern that complements that of Eps8. In the cochlea, whereas Eps8 is essential for the initial elongation of stereocilia, Eps8L2 is required for their maintenance in adult hair cells. In the absence of both proteins, the ordered staircase structure of the hair bundle in the cochlea decays. In contrast to the early profound hearing loss associated with an absence of Eps8, Eps8L2 null-mutant mice exhibit a late-onset, progressive hearing loss that is directly linked to a gradual deterioration in hair bundle morphology. We conclude that Eps8L2 is required for the long-term maintenance of the staircase structure and mechanosensory function of auditory hair bundles. It complements the developmental role of Eps8 and is a candidate gene for progressive age-related hearing loss.

deafness | sensory system | ion channel

Hearing and balance depend on the transduction of mechanical stimuli into electrical signals. Transduction involves activation of mechanically gated ion channels near the tips of the stereocilia, specialized microvilli that form the hair bundles that project from the surface of sensory hair cells (1). Stereocilia have a cytoskeletal core composed of tightly packed, cross-linked, and uniformly polarized actin filaments (2, 3). Stereociliary length is regulated to ensure the characteristic staircase-like structure of each bundle, whose overall size and shape depends on location along the sensory organ (4). In the mammalian cochlea, hair bundles usually include three rows of stereocilia coupled by several types of extracellular links (2, 5). The embryonic and postnatal development of the bundle involves elongation and thickening of stereocilia, as well as elimination of redundant stereocilia (4, 5).

In the adult cochlea, the height of stereocilia within each row is similar, not only within a single hair bundle but also between the bundles of adjacent hair cells, indicating a sophisticated level of control over growth (5, 6). Stereociliary growth and maintenance involves actin-binding proteins such as espin (7, 8), plastin (9), twinfilin 2 (10), gelsolin (11), and unconventional myosin motors including myosin XVa (12) and myosin IIIa (13). Currently, we do not have a complete molecular understanding of hair bundle structure or how its growth and maintenance are controlled. Recently, we showed that epidermal growth factor receptor pathway substrate 8 (Eps8) (14) is located at the tips of stereocilia where it regulates normal growth of the hair bundle (15, 16). In mammals, the Eps8 family includes three Eps8-related proteins named Eps8L1–L3. Eps8L1 and L2 also show actin binding activity, displaying similar domain organization and 27–42% identity to Eps8 (17). Eps8L2 shares a common modular protein structure to Eps8, indicating a possible overlap in function (17). However, despite the identification of Eps8L2 several years ago, its function remains unknown. Given that Eps8L2 has a remarkably similar expression pattern to that of Eps8, we hypothesized that it may be important for the growth and/or maintenance of hair cell stereocilia. We generated Eps8L2 KO mice and studied the structure and physiology of their mechanosensory systems. We found that the mice have progressive hearing loss, which is associated with progressive disorganization of cochlear hair bundles and abnormal variations in the length and width of stereocilia. We conclude that Eps8L2 is a newly identified stereociliary protein critical for hearing and for the normal function of mechanosensory hair bundles in adult mammals.

Results

Generation of Eps8L2 KO Mice. Eps8L2 KO mice were generated by replacing the exons encoding the SH3 domain (exons XVI and XVII) with a neomycin cassette (Fig. S1*A*). Targeted ES cells were identified by PCR (Fig. S1*B*), and correct insertion was verified at the 5′ and 3′ ends of the targeting vector by PCR and Southern blotting, respectively (Fig. S1 *C* and *D*). Injection of two correctly targeted ES cells into blastocysts gave rise to offspring with high coat chimaerism in both cases. Chimaeras were bred for germ-line transmission, and the resulting heterozygous mice were intercrossed to obtain Eps8L2 KO mice, which were

Author contributions: P.P.D.F., G.P.R., B.K., and W.M. designed research; D.N.F., S.L.J., U.M., L.R., A.T., N.O., J.O., R.J.G., S.V., Y.D., C.M.H., C.F., S.M.J., and W.M. performed research; D.N.F., S.L.J., U.M., L.R., A.T., N.O., J.O., R.J.G., S.V., Y.D., C.F., S.M.J., M.K., G.P.R., and W.M. analyzed data; and S.M., M.C.H., G.P.R., B.K., and W.M. wrote the paper.

The authors declare no conflict of interest.

This article is a PNAS Direct Submission. M.D. is a guest editor invited by the Editorial Board.

Freely available online through the PNAS open access option.

[1]D.N.F., S.L.J., U.M., and L.R. contributed equally to this work.

[2]Present address: KtedoGen srl, 20138 Milan, Italy.

[3]To whom correspondence should be addressed. E-mail: w.marcotti@sheffield.ac.uk.

This article contains supporting information online at www.pnas.org/lookup/suppl/doi:10.1073/pnas.1304644110/-/DCSupplemental.

born and weaned at the expected Mendalian ratio (Fig. S1*E*). Absence of Ep8L2 protein in lung tissue from Eps8L2 KO mice was verified by Western blotting (Fig. S1*F*).

Eps8L2 Is Localized at the Tips of Hair Cell Stereocilia. Immunofluorescence showed that Eps8L2 was expressed at the tips of cochlear hair cell stereocilia (Fig. 1; Fig. S2) and that it was absent in hair cells from Eps8L2 KO mice (Fig. S2). The distribution of Eps8L2 overlapped with that of Eps8 (15, 16) as previously suggested in other systems (17). However, the spatiotemporal expression patterns in cochlear hair cells were different. Eps8 labeling in the shortest rows of stereocilia diminished quickly during postnatal maturation but remained high in the longest row, whereas Eps8L2 labeling was high in the middle and shortest rows of fully grown stereocilia and was hardly detectable in the longest rows (Fig. 1*A*). The differential distribution of each protein to different rows of stereocilia was present as early as P2 (Fig. 1*B*), and it appeared to intensify with age and location along the cochlea (Fig. 1*A*). In vestibular hair, Eps8 and Eps8L2 were more obviously colocalized at the tips of most stereocilia in similar length-proportional amounts (Fig. 1*C*). Exogenous expression of GFP-Eps8L2 in the rat vestibular system (Fig. 1*D*) confirmed these results. However, similar to Eps8, we found that overexpression of Eps8L2 did not alter stereocilia length, suggesting that the activity of both proteins is likely to depend on other limiting factors, including the saturation of available binding sites by the endogenous protein.

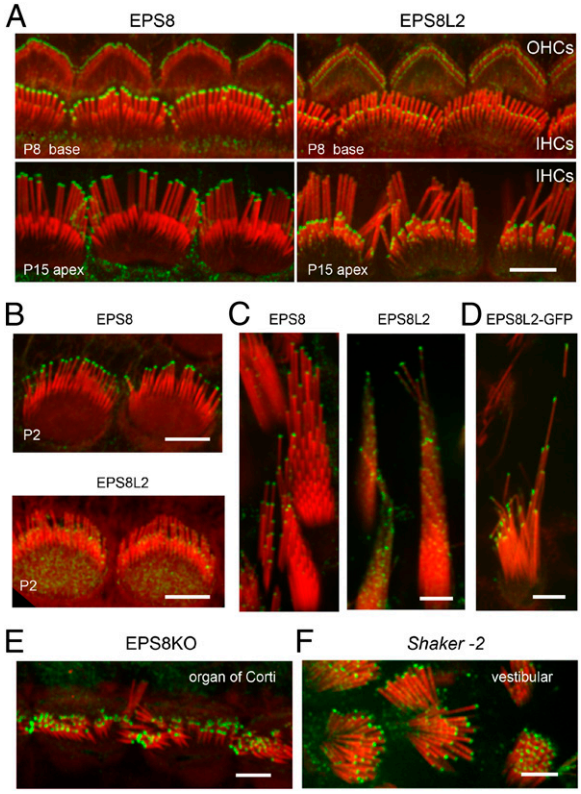

Fig. 1. Eps8L2 and Eps8 localize to stereocilia tips. (*A*) Monoclonal antibody for Eps8 (*Left*, green) and Eps8L2 (*Right*, green) shows localization at stereocilia tips in basal and apical hair cells from P8 and P15 rats. Phalloidin (red) is a stereocilia marker. (*B*) Immunofluorescence in rat IHCs shows Eps8 and Eps8L2 at the tips of immature (P2) stereocilia. (*C*) Eps8 and Eps8L2 localize to the tips of rat vestibular hair cell stereocilia. (*D*) Hair cells fixed 24 h after gene gun–mediated transfection of GFP-Eps8L2 in vestibular hair cells from neonatal rats display GFP-Eps8L2 localization at the tips of stereocilia in a similar pattern to the immunolocalization in *C*. (*E* and *F*) Eps8L2 localization to stereocilia tips is independent of Eps8 (*E*: Eps8 KO mouse hair cells) and myosin XVa (*F*: mouse *shaker-2* hair cells, which lack myosin XVa). (Scale bars, 5 μm.)

Eps8L2 remained at the tips of all cochlear hair cell stereocilia in Eps8 KO mice (Fig. 1*E*), which are short and show a relatively similar height among rows (15, 16). Despite the similar expression profile and high homology of the two genes (17), there is very little functional redundancy between the two proteins in cochlear hair cells. Although the localization of Eps8 requires the motor protein myosin XVa (15, 16), we found that in shaker-2 mice, which are deficient in myosin XVa (18), Eps8L2 was still present at the stereocilia tip (Fig. 1*F*).

Progressive Hearing Loss in Eps8L2 KO Mice. Eps8L2 KO mice (males and females) have progressive hearing loss, in contrast to the early profound hearing loss that occurs in the absence of Eps8. Auditory brainstem responses (ABRs) reflect the activity of the afferent auditory neurons downstream of the inner hair cells (IHCs). WT Eps8L2 littermates had normal thresholds for click, noise, and pure-tone evoked ABRs at about 2 mo of age (Fig. 2 *A–C*) and at 5–7 mo of age (Fig. 2 *D–F*). The thresholds for click stimuli were 18.3 ± 2.9 dB SPL at 2 mo, 16.5 ± 4.5 dB SPL at 5 mo, and 16.5 ± 3.9 dB SPL at 7 mo. Two-month-old Eps8L2 KO mice had significantly higher ABR thresholds for click (Fig. 2*A*), noise burst (Fig. 2*B*), and pure tone stimuli (Fig. 2*C*) above 4 kHz compared with control WT mice. The higher thresholds correlate with reduced ABR-wave amplitudes for all waves in the average ABR (Fig. S3 *A* and *B*). Input/output (I/O) functions increased monotonically in the majority of waves (Fig. S3*C*), and the latencies of the peaks were prolonged (Fig. S3*D*). By 5 mo of age, the ABR thresholds for click stimuli in Eps8L2 KO mice were even higher (Fig. 2 *D–F*). For pure-tone stimuli with frequencies >22 kHz, even with stimulus levels of 110 dB SPL, ABRs were not evoked in Eps8L2 KO mice (Fig. 2*F*). In 7-mo-old Eps8L2 KO mice, hearing thresholds increased yet further (Fig. 2*D*). Thus, the absence of Eps8L2 leads to a severe hearing loss in young adults.

Outer hair cell activity was studied by recording the amplitude and threshold of distortion product otoacoustic emissions (DPOAEs; Fig. S4 *A–F*). In 2-mo-old Eps8L2 KO mice, DPOAE amplitudes at 50 dB SPL stimulus level were similar to those of control WT mice (Fig. S4*A*). However, DPOAE thresholds at higher stimulus frequencies (22.6 and 32 kHz; Fig. S4*B*) were higher in Eps8L2 KO mice. In 5-mo-old Eps8L2 KO mice, DPOAE amplitudes were lower at nearly all stimulus levels (Fig. S4 *D* and *F*), and DPOAE thresholds were significantly higher for stimulus frequencies at and above 11.3 kHz (Fig. S4*E*), indicating an age-related loss of outer hair cell (OHC) function.

To discover if threshold elevation in Eps8L2 KO mice at younger ages resulted from an alteration in auditory nerve transduction, we recorded compound action potentials (CAPs), which reflect activity of auditory afferent fibers, and summating potentials (SPs), which reflect IHC depolarization (Fig. S4 *G–L*). Thresholds for click-evoked CAPs were about 32 dB higher in Eps8L2 KO mice compared with WT littermates (Fig. S4*G*). During pure tone stimulation, Eps8L2 KO mice had higher thresholds for tones above 4 kHz and no responses above 8 kHz (Fig. S4*A*). SP thresholds were elevated at all frequencies tested (Fig. S4*I*). The results indicate that in Eps8L2 KO mice, the generation of receptor potentials in hair cells at lower sound pressure levels is impaired, which leads to a reduction in auditory nerve responses.

Vestibular-Evoked Potentials in Eps8L2 KO Mice. We investigated the vestibular-evoked potential (VsEP) waveforms (Fig. S5*A*) from Eps8L2 control and KO mice between 2 and 3 mo of age, a time at which auditory defects are already evident (Fig. 2). VsEP thresholds were similar between heterozygous control (−9.00 ± 2.77 dB) and KO mice (−9.10 ± 3. 39 dB) at levels aligned with normal mice (19), which suggests that the general sensitivity of the vestibular organs is not impacted by the absence of Eps8L2. P1 latencies (Fig. S5*B*), but not the P1-N1 amplitudes (Fig. S5*C*), were significantly (ANOVA: $P < 0.003$) prolonged in KO mice compared with control littermates, indicating that the absence of

GENETICS

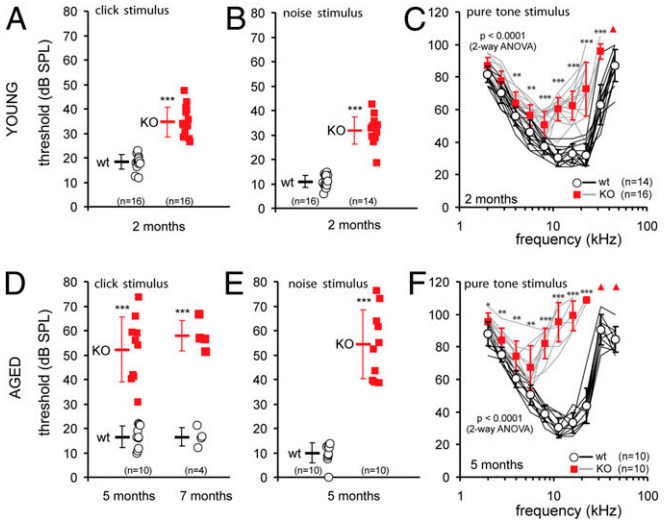

Fig. 2. ABRs in young and aged Eps8L2 mice. (*A–C*) ABR thresholds obtained from control (16 ears from eight mice: circles and black line) and Eps8L2 KO (14–16 ears from eight mice: red squares and red line) 2-mo-old mice (P41–P66). ABR thresholds for broadband click (*A*), broadband noise burst stimuli (*B*), and frequency-specific pure tone stimulation of 4 kHz and above (*C*) in Eps8L2 KO mice were significantly higher than those in control mice. For 45-kHz stimuli, no response could be measured in Eps8L2 KO mice even with the highest stimulus SPL. (*D–F*) ABR thresholds for 5-mo-old mice (P153–P157) and 7-mo-old mice. Eps8L2 KO mice were significantly increased for click (*D*), noise burst (*E*), and pure tone stimuli of 2 kHz and above (*F*). At and above 32 kHz, no response could be evoked with the highest stimulus SPL (*F*). ABR for click stimuli were also performed in 7-mo-old mice (*D*). Thresholds of individual ears are shown as circle and square symbols (click and noise) and gray lines (pure tone). Asterisks indicate statistical significance: $*P < 0.05$, $**P < 0.01$, $***P < 0.001$. Horizontal bars (*A, B, D,* and *E*) and circle and square symbols (*C* and *F*) give the mean ± SD. Number of ears tested shown in parentheses.

Eps8L2 causes a subtle vestibular phenotype that impacts on the neural activation of vestibular primary afferents. A similar phenotype (prolonged P1 latencies in VsEPs) has been shown, although with much stronger effect, for other stereociliary mutant mice such as *Ptprq* mice (20).

Mechanotransducer Currents and Basolateral Membrane Properties in Eps8L2 KO Mice. Given the location of Eps8L2 at the stereociliary bundles from early stages of development, we investigated its possible role in mechanotransduction. Mechanotransducer (MET) currents were recorded from immature OHCs by displacing their hair bundles using a fluid-jet (21). Bundle displacement in the excitatory direction (i.e., toward the taller stereocilia) at negative membrane potentials elicited a similar maximal inward MET current in control (−1,577 ± 151 pA, $n = 5$) and KO (−1,617 ± 139 pA, $n = 5$) OHCs (Fig. 3 *A* and *B*). The resting MET current was reduced when bundles were moved in the inhibitory direction (Fig. 3 *A* and *B*, arrowheads). The current became outward when excitatory bundle stimulation was applied during voltage steps positive to the reversal potential of the MET current (near 0 mV: Fig. 3*C*). The normal MET current in Eps8L2 KO mice correlates with the hair bundle structure, which appears similar to that of the control (Fig. 3 *A* and *B*, *Upper*). We tested whether the MET current was present in adult hair cells by using the styryl dye FM1-43, a dye that has previously been used to assess the presence of the resting transducer current (22). Bath application of FM1-43 labeled both control and Eps8L2 KO adult hair cells (P22–P30; Fig. 3*D*). The generation of the Eps8/Eps8L2 double KO further supported the evidence that Eps8L2 is not required for MET in immature OHCs (Fig. 3*E*), because their reduced resting current, mainly evident at +98 mV (Fig. 3*E*, *Lower*, arrow), resembled that observed when only Eps8 was absent (Fig. 3*E*, *Upper*) (16).

We studied the basolateral membrane properties in hair cells from Eps8L2 KO mice to determine whether the loss of auditory function was associated with abnormalities in basolateral membrane properties, as previously seen in the absence of Eps8 (16). These studies revealed no differences in the K^+ currents in control and Eps8L2 KO IHCs at P18 and P96, the expression of the motor protein prestin in P135 OHCs (Fig. S6 *A–D*), or resting membrane potential (control IHCs: −77 ± 1 pA, $n = 9$; KO: −76 ± 1 pA, $n = 11$). These findings indicate that hair cells do not degenerate in adult Eps8L2 KO mice, a finding also supported by the presence of normal-looking organ of Corti in adult mice (Fig. S6 *E* and *F*).

Hair Cells from Eps8L2 KO Mice Show Progressive Hair Bundle Deterioration. Eps8L2 KO hair bundles appeared to be normal in early development, whereas those in Eps8 KO mice are characteristically short. We hypothesized that progressive hearing loss in Eps8L2 KO mice is due to gradual deterioration of the hair bundle structure. Scanning electron microscopy (SEM) showed that hair bundles in Eps8L2 KO mice at 1 mo were superficially similar to those in littermate controls (Fig. 4 *A* and *B*). However, a few abnormally long stereocilia were visible in the middle row (Fig. 4*B*, arrows), and some stereocilia were shorter or missing (Fig. 4*B*, arrowheads). Similar short or missing stereocilia have previously been described in null mice for γ-actin (23). Despite these abnormalities, hair bundles from Esp8L2 KO mice possessed tip links (Fig. S6*G*) and expressed several proteins that normally form the tip link core (cdh23 and pcdh15) and shaft connectors (ptprq; Fig. S7) (5). At 3 and 8 mo (Fig. 4 *C* and *D* and *E* and *F*, respectively), there was evidence for progressive deterioration of bundles in both IHCs and OHCs of Esp8L2 KO mice. The most obvious abnormalities included a larger number of shorter or missing stereocilia, especially in OHCs (Fig. 4 *D* and *F*, arrowheads), and a shallower hair bundle staircase architecture, which was more pronounced in IHCs. Loss of the staircase structure was apparently due to greater variability in stereociliary height within the intermediate and shorter rows. There were also abnormally long stereocilia in the IHCs. These defects were more pronounced toward higher-frequency regions of the cochlea (Fig. 4*G*: ∼4 kHz; Fig. 4*H*: ∼15 kHz), consistent with the increased hearing loss in this region (Fig. 2). We quantified these differences by measuring stereocilia number, height, and width at P90. The number of stereocilia in apical IHCs was significantly lower ($P < 0.02$) in Eps8L2 KO mice (39 ± 4, $n = 7$) than in controls (45 ± 3, $n = 7$). The height of individual stereocilia in IHCs was measured without categorizing them into rows beforehand (tall, intermediate, or short) because, although possible in controls (Fig. 4 *C* and *E*), it was difficult to define them with precision in the Eps8L2 KOs (Fig. 4 *D* and *F*). Fig. 4 *I–K* shows examples of stereocilia height within hair bundles in three control and four KO P90 IHCs, respectively. In the absence of Eps8L2, the tall stereocilia were shorter and fewer than those of the controls. However, there was little difference between the heights of stereocilia in the intermediate and short rows, with the latter approaching the length of intermediate stereocilia and thus partially compromising the staircase architecture (Fig. 4 *I–K*). The widths of individual stereocilia were measured at ∼20% from their tips, which corresponds to the widest section for control intermediate stereocilia. For each hair bundle, only stereocilia that could be clearly identified as intermediate were measured. In IHCs from KO mice, the intermediate stereocilia were significantly narrower ($P < 0.0001$) than in the controls (Fig. 4*L*). The width ratio between the tall and intermediate stereocilia was about 1 in control and 1.8 in Eps8L2 mutant hair bundles. Intermediate stereocilia in KO mice also tended to have an irregular shape, including thinning at the distal end (Fig. 4*I*). These abnormalities were accentuated by P240 (Fig. 4*F*). Despite the defects associated

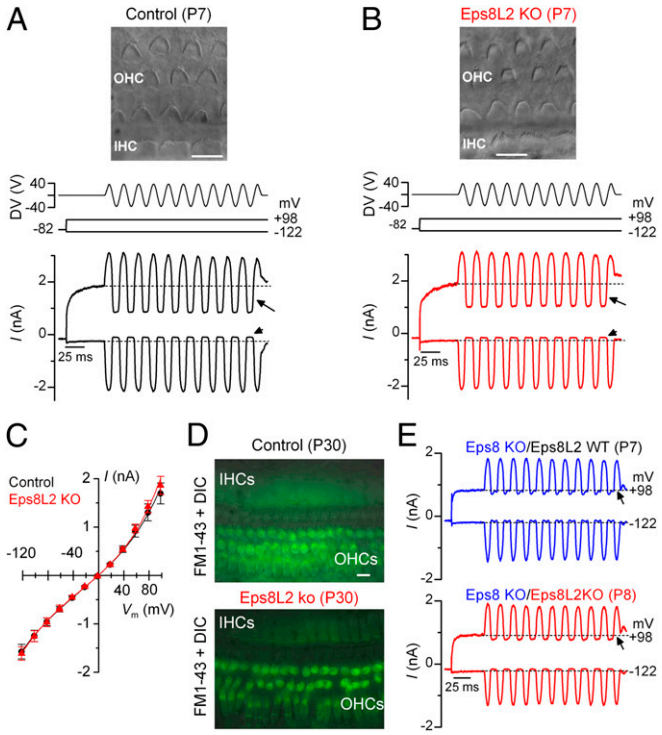

Fig. 3. Mechanotransducer currents in Eps8L2 cochlear hair cells. (*A* and *B*) Saturating transducer currents recorded from a control (*A*) and a KO (*B*) Eps8L2 OHC by applying sinusoidal force stimuli of 50 Hz to the hair bundles. The driver voltage (DV) signal to the fluid jet is shown above the traces (negative deflections of the DV are inhibitory). The membrane potential was stepped between −122 and +98 mV in 20-mV nominal increments from −82 mV. For clarity only a few responses are shown. The arrowheads and arrows indicate the closure of the transducer channel elicited during inhibitory bundle displacements. Note that the resting current increases with membrane depolarization. The upper panels show interference contrast microscopy images of the hair cell hair bundles taken from the experimental microscope. (Scale bars, 10 μm). (*C*) Peak-to-peak current-voltage curves were obtained from five control and five KO P7 OHCs. (*D*) Fluorescence images with the DIC image superimposed from the control and KO cochleae taken after exposure to FM1-43 (both OHCs and IHCs were labeled by the dye). (Scale bars, 20 μm.) (*E*) Saturating transducer currents recorded from an Eps8-KO/Eps8L2-WT (*Upper*) and an Eps8-KO/Eps8L2-KO OHC using the same protocol described in *A* and *B*.

with the absence of Eps8L2, the staircase-like architecture of hair bundles was partially preserved even though it became shallower with age. The hair bundle abnormalities in both IHCs and OHCs were strongly enhanced in the Eps8/Eps8L2 double KO mice (Fig. S8), with hair bundles showing a profound disorganization and a complete absence of the staircase-like architecture. In contrast, the height of stereocilia and bundle morphology of vestibular hair cells was not obviously affected by the absence (Fig. S5 *D–G*: adult mice) or the exogenous expression (Fig. 1*D*: immature mice) of Eps8L2, which is also consistent with the mild phenotype observed in the VsEPs measured in Eps8L2 KO animals (Fig. S5 *A–C*).

Transmission electron microscopy (TEM) showed that the actin filaments within stereocilia and the cross-links between stereocilia appeared to be organized normally in Eps8L2 KO mice at P25. However, at P240, the diameters of stereocilia within a single row in Eps8L2 KO mice were very variable but with normal actin filament packing (Fig. S9 *A–E*). Although it is more difficult with TEM to know the exact position along the length of the shaft of each stereocilium, the width ratio between the tall and intermediate stereocilia (controls, ∼1; Eps8L2 mutants, 1.3) suggested that stereocilia were thinner in mutants, thus further supporting the measurements in SEM. Thus, in the absence of Eps8L2 in the stereocilia there is a loss in regulation of the number of parallel actin filaments. TEM images also revealed a significantly reduced cuticular plate thickness in hair cells from 240-d-old Eps8L2 KO mice compared with littermate controls (Fig. S9 *F–J*), which is consistent with Eps8L2 expression at this location (Fig. 1 *A* and *B*). Therefore, some hair bundle disruption in Eps8L2 KO mice could also reflect the reduced anchoring in the cuticular plate.

Discussion

The Eps8 family of actin regulatory proteins includes four members, Eps8 and the three Eps8-like variants Eps8L1, Eps8L2, and Eps8L3, which appear to have partially overlapping functions in regulating actin cytoskeletal networks. Eps8L2 is structurally the most closely related to Eps8 and shares very similar expression patterns, suggesting some level of redundancy in most tissues (17). We have shown that Eps8L2 is expressed at the apical ends of hair cells and at the tips of mechanosensory stereocilia in mammalian inner ear hair cells. We propose that Eps8L2 has a distinct, complementary function to that of Eps8 in regulating hair-bundle structure and maintenance. Eps8L2 KO mice suffer from progressive hearing loss that reflects a gradual, late-onset deterioration in hair-bundle structure. In contrast, mice lacking Eps8 are profoundly deaf from the onset of hearing (16). The normal development and maintenance of hair bundles requires differential regulation of actin filaments in stereocilia of different length within one bundle and between hair bundles on adjacent hair cells (2, 24, 25). The mechanical properties of stereocilia are also a function of combinations of actin-binding proteins (26). In cochlear hair cells, bundle length generally increases incrementally toward the apical, low-frequency end of the auditory epithelium (27). Hair bundles include numerous cytoskeletal proteins and mutations in many of them cause a wide range of morphological and functional defects (5, 6, 28). These proteins include motor proteins such as myosin VIIa (29) and myosin XVa (30), actin cross-linking proteins such as espin (7), the actin-binding scaffold protein harmonin-b (31), and actin filament capping proteins such as twinfilin 2 (10), gelsolin (11), Eps8 (15, 16), and now Eps8L2.

Eps8L2 and Eps8 Have Distinct and Complementary Subcellular Distributions. We found that Eps8 and Eps8L2 have complementary overlapping distributions in stereocilia. In cochlear hair cells, Eps8L2 is expressed most prominently at the tips of the short and intermediate rows of stereocilia, whereas Eps8 is most prominent in the longest rows. Although Eps8L2 is expressed in the taller stereocilia of vestibular hair cells, similar to Eps8, the relationship with length is less pronounced. Our results also show that the location of Eps8L2 is independent not only of Eps8 but also of MyoXVa, a protein required for the tip localization of Eps8 (15). MyoXVa may enhance the actin-binding potential of Eps8 relative to Eps8L2 in longer stereocilia or Eps8L2 might be translocated differentially by another myosin isoform, such as MyoIIIa or MyoVIIa (4). Alternatively, Eps8L2 could passively diffuse along the length of stereocilia and accumulate at their tips by binding to actin filament barbed ends or other binding partners.

Loss of Eps8L2 Is Associated with Severe Progressive Hearing Loss as Opposed to Profound Deafness. During development, hair cell bundles from Eps8L2 KO mice seem to grow normally and to develop the characteristic staircase architecture with mechanosensory tip links. The normal hair bundle morphology was consistent with the presence of normal MET currents during immature stages of development. Furthermore, we found no evidence for deficits in the development of basolateral membrane properties in cochlear hair cells. In contrast, deletion of Eps8 compromises all of these aspects of cell differentiation and prevents hair cell maturation, which may be a downstream consequence of the transduction defects that are detected from an early age (16). The lack of a more severe phenotype in the Eps8L2 KO mouse could be explained by functional redundancy with Eps8L1 or Eps8L3 (14), but there is no evidence that these proteins are expressed in hair cells.

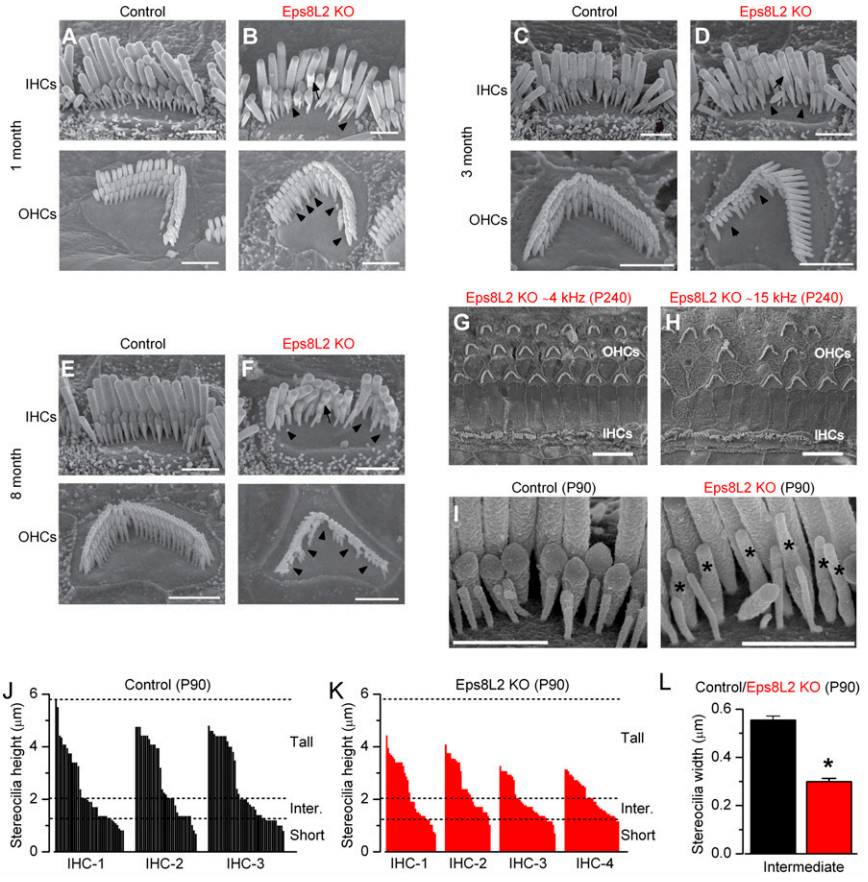

Fig. 4. Hair bundle morphology in hair cells from adult Eps8L2 mice. (*A–F*) SEM showing the typical hair bundle structure from apical-coil IHCs and OHCs in control (*A*, *C*, and *E*) and Eps8L2 KO (*B*, *D*, and *F*) mice of increasing age (1, 3, and 8 mo). Note that generally, hair bundles are composed of three rows of stereocilia: tall, intermediate, and short. (Scale bars, 2 μm; different magnifications have been used in all panels.) Arrowheads indicate missing stereocilia. Arrows indicate some misplaced tall stereocilia. (*G* and *H*) Low-magnification SEM images showing hair bundles from IHCs and OHCs located at two different frequency regions along the cochlea (~4 and ~15 kHz, respectively) of Eps8L2 KO mice at 8 mo. (Scale bar, 10 μm.) Note that the number of missing OHC hair bundles at ~15 kHz is greater than that at ~4 kHz. (*I*) SEM images showing the shape of intermediate stereocilia in control and Eps8L2 KO P90 IHCs. Note that in KOs, the intermediate stereocilia were thinner than those in controls and have a bulbous widening at various distances along the shafts (asterisks mark stereocilia with abnormal shape). (Scale bars, 2 μm.) (*J* and *K*) Distribution of stereocilia height in three control and four KO Eps8L2 IHCs. Note that KO IHCs showed a reduced height of the taller stereocilia and a less defined separation between the three stereocilia rows. (*L*) Stereociliary width of intermediate stereocilia in control and KO Eps8L2 IHC hair bundles (each average was obtained from about 20 stereocilia from four IHC hair bundles). The width was measured at ~20% from the tip of the stereocilia, which corresponds to the widest section in control stereocilia.

Function of Eps8L2 in the Maturation and Maintenance of Stereocilia. The gradual degradation of the cochlear hair bundle structure in Eps8L2 KO mice is associated with progressive hearing loss, especially at higher frequencies. In adult Eps8L2 KO mice, the most striking observation is the substantially reduced staircase organization of the hair bundles. The longest stereocilia are about 30% shorter than normal, whereas the intermediate and short stereocilia show a wide range in length, with some being abnormally long. These defects are less evident in OHCs in which there is a substantial loss of intermediate and shorter stereocilia with age. Thus, the phenotypes of the hair bundles in the Eps8L2 KO and the EPS8 KO described previously (16) are different. Despite the presence of Eps8L2 in the stereocilia of vestibular hair cells, Eps8L2 KO mice showed a very mild functional vestibular phenotype (Fig. S5). This was consistent with the normal hair bundle morphology in vestibular hair cells of Eps8L2 KO mice, which could reflect their generally less tightly organized hair bundles compared with those of the cochlear hair cells and/or the stronger selection for redundancy in vestibular organs. Indeed, genetic mutations affecting both cochlear and vestibular stereocilia structure and function are very often associated with nonsyndromic deafness (28), suggesting that vestibular hair cells have greater resistance to loss of regulatory components, which may in turn indicate stronger selective pressure for balance (survival and reproduction) vs. hearing.

Eps8 and Eps8L1-L3 (14) are endowed with multiple functions in the control of actin dynamics. Depending on their association with other signal transducers, they act directly on actin by binding to it and by modulating actin bundling and/or actin barbed-end capping activities (32–34). Notably, Eps8L2 lacks IRSp53 binding, which is essential in Eps8 for relieving inhibition of actin-bundling activity (33). Interestingly, in the gut brush border cells, Eps8 activity lengthens microvilli (35), whereas Eps8L1 shortens them (36). A similar mechanism could be present in hair cell stereocilia, where Eps8 would mainly favor the elongation of the taller stereocilia (15, 16). In the adult cochlea, Eps8L2 could restrict elongation of the intermediate and shorter stereocilia (Fig. 4) by capping the barbed ends of actin filaments, a role proposed for twinfilin 2 during early stereocilia growth (10). Although the measured turnover of actin in mature stereocilia is very slow, possibly to ensure that the staircase structure established during development persists through adult life, there is a region of relatively high actin turnover at the tip of each stereocilium (37). Turnover in this region may be regulated by Eps8L2, possibly in response to extrinsic physiological signals, as indicated by its molecular structure (17). Actin turnover would enable the fine-tuning of the staircase structure and could explain why Eps8L2 seems not to play a crucial role in hair bundle growth. Instead it may provide a balance between the conflicting needs for structural stability and the repair or renewal of structures at the stereociliary tip, not least those of the tip link anchorage. Eps8 could have a similar function in the longer stereocilia, possibly by acting as a "gated-capper" protein (15), in which it protects the actin barbed end from other capping proteins but allows those promoting elongation, such as espin (8, 38).

Eps8L2 in Bundling of Actin Filaments. The absence of Eps8L2 also results in a reduction in stereociliary diameter, a phenotype not seen in Eps8 KO mice. The normal increase in stereociliary width during development, and its maintenance thereafter, is thought to arise from the addition of actin filaments to the periphery of the existing actin core (2). Although the absence of Eps8L2 results in a wide variability in stereocilia diameter, the density of actin filaments seems unaffected, indicating that the overall number of filaments is altered. In addition, we observed a tapering at the distal ends of stereocilia, similar to the slowing in the peripheral growth of parallel actin filaments seen in mice with a mutation in the actin cross-linking protein espin (8).

Although this suggests a role for Eps8L2 in actin bundling, it does not bind IRSp53, a protein essential for Eps8 actin-bundling activity in vivo (33). The interaction partners of Esp8L2 in hair cells are unknown, so an actin bundling role for Eps8L2, as suggested by the observed "candlewick" tapering of the distal tips of second and third row stereocilia, should not be excluded in hair–cell systems.

Although Eps8 and Eps8L2 are structurally complementary, they have different roles: whereas Eps8 is involved in stereociliary growth, Eps8L2 is essential for the stability of hair bundles once they have formed. Together, the two proteins contribute to the normal development and maintenance of hair bundle architecture. Progressive hearing loss in Eps8L2 KO mice indicates that Eps8L2 is a candidate gene for presbycusis, together with other known molecules such as the potassium channel *KCNQ4* (39) and the glutamate receptor *GRM7* (40).

Materials and Methods

A detailed description of the different methods is available as *SI Materials and Methods*.

Generation of Eps8L2 KO Mice. Eps8L2 KO mice were generated by deleting the two exons (XVI–XVII) that code for the SH3 domain of the protein. The targeting vector contained a neomycin cassette (retained in the KO) and a diphtheria toxin A cassette for negative selection.

Immunostaining. Cochleae from immature and mature Eps8L2 and Eps8 mice were fixed with 2% or 4% (vol/vol) paraformaldehyde (PFA) for 2 h. Eps8L2 antibody (a rabbit polyclonal) was raised against a glutathion-S-transferase–fusion protein containing amino acids 547–715 of human Eps8L2 (NP_073609.2) and immunopurified.

In Vivo Hearing Tests and Electrocochleography. All in vivo measurements (ABRs, DPOAEs, and CAPs) were performed on eight WT and eight KO Eps8L2 mice between 2 and 7 mo of age. All recordings were performed under anesthesia, and the experimental protocols were reviewed and approved by the animal welfare commissioner and the regional board for scientific animal experiments in Tübingen (Germany).

In Vivo VsEPs. All in vivo measurements on Eps8L2 mice were performed on nine KO and nine heterozygous control littermates between 2 and 3 mo of age. The use of animals was approved by the University of Nebraska Lincoln Institutional Animal Care and Use Committee.

Single Hair Cell Electrophysiology. Patch-clamp recordings were performed from IHCs and OHCs of Eps8L2 and Eps8 KO mice (P7–P96) and their control littermates. Mice were killed by cervical dislocation in accordance with UK Home Office regulations. Statistical comparisons of means were made by Student two-tailed *t* test or, for multiple comparisons, ANOVA, usually one-way ANOVA followed by the Tukey test. Mean values are quoted ±SEM, where $P < 0.05$ indicates statistical significance.

SEM and TEM. Cochleae from control and KO Eps8L2 mice were fixed for 2 h with 2.5% (vol/vol) glutaraldehyde.

ACKNOWLEDGMENTS. We thank Choongheon Lee for assistance with VsEP data collection. This work was supported by the following grants: Wellcome Trust (091895) and Westfield Health (W.M.), the fondazione cariplo (2012/5746) (to W.M. and S.M.), the Wellcome Trust (087737) (to G.P.R.), Deutsche Forschungsgemeinschaft DFG Kni 316-4-1 (to M.K.), the Intramural Programs of the National Institute on Deafness and Other Communication Disorders (B.K.), and the Nebraska Tobacco Settlement Biomedical Research Development Fund (to S.M.J.). S.L.J. is a Royal Society University Research Fellow.

1. Fettiplace R, Hackney CM (2006) The sensory and motor roles of auditory hair cells. *Nat Rev Neurosci* 7(1):19–29.
2. Tilney LG, Tilney MS, DeRosier DJ (1992) Actin filaments, stereocilia, and hair cells: How cells count and measure. *Annu Rev Cell Biol* 8:257–274.
3. Bartles JR (2000) Parallel actin bundles and their multiple actin-bundling proteins. *Curr Opin Cell Biol* 12(1):72–78.
4. Manor U, Kachar B (2008) Dynamic length regulation of sensory stereocilia. *Semin Cell Dev Biol* 19(6):502–510.
5. Petit C, Richardson GP (2009) Linking genes underlying deafness to hair-bundle development and function. *Nat Neurosci* 12(6):703–710.
6. Schwander M, Kachar B, Müller U (2010) Review series: The cell biology of hearing. *J Cell Biol* 190(1):9–20.
7. Zheng L, et al. (2000) The deaf jerker mouse has a mutation in the gene encoding the espin actin-bundling proteins of hair cell stereocilia and lacks espins. *Cell* 102(3):377–385.
8. Sekerková G, Richter CP, Bartles JR (2011) Roles of the espin actin-bundling proteins in the morphogenesis and stabilization of hair cell stereocilia revealed in CBA/CaJ congenic jerker mice. *PLoS Genet* 7(3):e1002032.
9. Daudet N, Lebart MC (2002) Transient expression of the t-isoform of plastins/fimbrin in the stereocilia of developing auditory hair cells. *Cell Motil Cytoskeleton* 53(4):326–336.
10. Peng AW, Belyantseva IA, Hsu PD, Friedman TB, Heller S (2009) Twinfilin 2 regulates actin filament lengths in cochlear stereocilia. *J Neurosci* 29(48):15083–15088.
11. Mburu P, et al. (2010) Gelsolin plays a role in the actin polymerization complex of hair cell stereocilia. *PLoS ONE* 5(7):e11627.
12. Belyantseva IA, et al. (2005) Myosin-XVa is required for tip localization of whirlin and differential elongation of hair-cell stereocilia. *Nat Cell Biol* 7(2):148–156.
13. Salles FT, et al. (2009) Myosin IIIa boosts elongation of stereocilia by transporting espin 1 to the plus ends of actin filaments. *Nat Cell Biol* 11(4):443–450.
14. Scita G, et al. (1999) EPS8 and E3B1 transduce signals from Ras to Rac. *Nature* 401(6750):290–293.
15. Manor U, et al. (2011) Regulation of stereocilia length by myosin XVa and whirlin depends on the actin-regulatory protein Eps8. *Curr Biol* 21(2):167–172.
16. Zampini V, et al. (2011) Eps8 regulates hair bundle length and functional maturation of mammalian auditory hair cells. *PLoS Biol* 9(4):e1001048.
17. Offenhäuser N, et al. (2004) The eps8 family of proteins links growth factor stimulation to actin reorganization generating functional redundancy in the Ras/Rac pathway. *Mol Biol Cell* 15(1):91–98.
18. Probst FJ, et al. (1998) Correction of deafness in shaker-2 mice by an unconventional myosin in a BAC transgene. *Science* 280(5368):1444–1447.
19. Mock BE, Jones TA, Jones SM (2011) Gravity receptor aging in the CBA/CaJ strain: A comparison to auditory aging. *J Assoc Res Otolaryngol* 12(2):173–183.
20. Goodyear RJ, Jones SM, Sharifi L, Forge A, Richardson GP (2012) Hair bundle defects and loss of function in the vestibular end organs of mice lacking the receptor-like inositol lipid phosphatase PTPRQ. *J Neurosci* 32(8):2762–2772.
21. Johnson SL, Beurg M, Marcotti W, Fettiplace R (2011) Prestin-driven cochlear amplification is not limited by the outer hair cell membrane time constant. *Neuron* 70(6):1143–1154.
22. Gale JE, Marcotti W, Kennedy HJ, Kros CJ, Richardson GP (2001) FM1-43 dye behaves as a permeant blocker of the hair-cell mechanotransducer channel. *J Neurosci* 21(18):7013–7025.
23. Belyantseva IA, et al. (2009) Gamma-actin is required for cytoskeletal maintenance but not development. *Proc Natl Acad Sci USA* 106(24):9703–9708.
24. Tilney LG, Tilney MS, Cotanche DA (1988) Actin filaments, stereocilia, and hair cells of the bird cochlea. V. How the staircase pattern of stereociliary lengths is generated. *J Cell Biol* 106(2):355–365.
25. Kaltenbach JA, Falzarano PR, Simpson TH (1994) Postnatal development of the hamster cochlea. II. Growth and differentiation of stereocilia bundles. *J Comp Neurol* 350(2):187–198.
26. Claessens MM, Bathe M, Frey E, Bausch AR (2006) Actin-binding proteins sensitively mediate F-actin bundle stiffness. *Nat Mater* 5(9):748–753.
27. Garfinkle TJ, Saunders JC (1983) Morphology of inner hair cell stereocilia in C57BL/6J mice as studied by scanning electron microscopy. *Otolaryngol Head Neck Surg* 91(4):421–426.
28. Drummond MC, Belyantseva IA, Friderici KH, Friedman TB (2012) Actin in hair cells and hearing loss. *Hear Res* 288(1-2):89–99.
29. Kros CJ, et al. (2002) Reduced climbing and increased slipping adaptation in cochlear hair cells of mice with Myo7a mutations. *Nat Neurosci* 5(1):41–47.
30. Stepanyan R, Frolenkov GI (2009) Fast adaptation and Ca^{2+} sensitivity of the mechanotransducer require myosin-XVa in inner but not outer cochlear hair cells. *J Neurosci* 29(13):4023–4034.
31. Michalski N, et al. (2009) Harmonin-b, an actin-binding scaffold protein, is involved in the adaptation of mechanoelectrical transduction by sensory hair cells. *Pflugers Arch* 459(1):115–130.
32. Disanza A, et al. (2004) Eps8 controls actin-based motility by capping the barbed ends of actin filaments. *Nat Cell Biol* 6(12):1180–1188.
33. Disanza A, et al. (2006) Regulation of cell shape by Cdc42 is mediated by the synergic actin-bundling activity of the Eps8-IRSp53 complex. *Nat Cell Biol* 8(12):1337–1347.
34. Hertzog M, et al. (2010) Molecular basis for the dual function of Eps8 on actin dynamics: Bundling and capping. *PLoS Biol* 8(6):e1000387.
35. Tocchetti A, et al. (2010) Loss of the actin remodeler Eps8 causes intestinal defects and improved metabolic status in mice. *PLoS ONE* 5(3):e9468.
36. Zwaenepoel I, et al. (2012) Ezrin regulates microvillus morphogenesis by promoting distinct activities of Eps8 proteins. *Mol Biol Cell* 23(6):1080–1094.
37. Zhang DS, et al. (2012) Multi-isotope imaging mass spectrometry reveals slow protein turnover in hair-cell stereocilia. *Nature* 481(7382):520–524.
38. Rzadzinska A, Schneider M, Noben-Trauth K, Bartles JR, Kachar B (2005) Balanced levels of Espin are critical for stereociliary growth and length maintenance. *Cell Motil Cytoskeleton* 62(3):157–165.
39. Van Eyken E, et al. (2006) KCNQ4: A gene for age-related hearing impairment? *Hum Mutat* 27(10):1007–1016.
40. Newman DL, et al. (2012) GRM7 variants associated with age-related hearing loss based on auditory perception. *Hear Res* 294(1-2):125–132.